33rd Annual International Conference of the IEEE EMBS
Boston, Massachusetts USA, August 30 - September 3, 2011

Automatic Glaucoma Diagnosis from Fundus Image

J. Liu, F. S. Yin, D.W.K. Wong, Z. Zhang, N.M. Tan, C. Y. Cheung, M. Baskaran, T. Aung and T.Y. Wong

***Abstract*— Glaucoma is currently diagnosed by glaucoma specialists using specialized imaging devices like HRT and OCT. Fundus imaging is a modality widely used in primary healthcare. An automatic glaucoma diagnosis system based on fundus image can be deployed to primary healthcare clinics and has potential for early disease diagnosis. A mass glaucoma screening program can also be facilitated using such a system. We present an automatic fundus image based cup-to-disc ratio measurement system; and demonstrate its potential for automatic objective glaucoma diagnosis and screening. It provides strong support to use fundus image as the modality for automatic glaucoma diagnosis.**

I. Introduction

Glaucoma [1] is a chronic and irreversible neurodegenerative eye condition in which the nerve that connects the eye to the brain (optic nerve) is progressively damaged. It is the second leading cause of blindness worldwide with estimated 60 million glaucoma cases globally in 2010 [2]. The management of glaucoma costs about $2.5 billion per year in US alone [3]. Unlike other eye diseases like cataract and myopia, glaucoma cannot be cured as the damage of the optic nerve is permanent, and any treatment is unable to restore vision. Early detection is thus essential for early treatment to prevent the deterioration of the vision [4]. However, a key challenge is that many glaucoma patients are not aware of their condition. In Singapore, the SIMES eye study [5] showed that 90% of the glaucoma patients are unaware of their conditions. That is why glaucoma is also called the "silent theft of sight". Furthermore, current glaucoma detection requires patient examination by glaucoma specialists (ophthalmologists with specialized glaucoma training) and requires expensive specialized equipment. There are no cost-effective glaucoma screening programs available currently. It is therefore critical and challenging to detect/diagnose glaucoma early using non-specialized equipment, particularly with minimal involvement from glaucoma specialists at the primary healthcare level. An early detection system has the potential to be deployed to primary healthcare clinics to detect glaucoma patients, who might not be aware of their conditions, during normal eye examinations. Glaucoma early detection using unspecialized equipment poses challenges to glaucoma research and management.

Clinically, the following three examinations are currently practiced to detect glaucoma:

a) Intraocular pressure (IOP) measurement
b) Visual field test
c) Optic nerve assessment

IOP is an important risk factor, however there are many glaucoma patients with normal tension. In the Rotterdam Eye Study, of the 104 cases of definite open-angle glaucoma, 33 had IOPs less than 22 mmHg in the involved eye [6]. IOP measurement is thus not specific enough to be an effective detection tool. Function-based visual field testing requires special equipments not normally present in the primary healthcare clinics, and the vision lost is often occurs after optic nerve structural damages and patients with early glaucoma often do not have visual symptoms (as shown in Fig. 1). Optic nerve assessment is thus able to detect glaucoma early and is currently performed by a trained glaucoma specialist, or using specialized expensive equipment such as the OCT (Optical coherence tomography) and HRT (Heidelberg Retinal Tomography) systems. However, optic disc assessment by an ophthalmologist is subjective and the availability of OCT/HRT is limited because of the cost involved. It has shown[7] that the inherent subjectivity of manual clinical assessment is subject to fairly large inter- and intra-observer variability in distinguishing between glaucomatous and normal optic nerve heads. Thus,

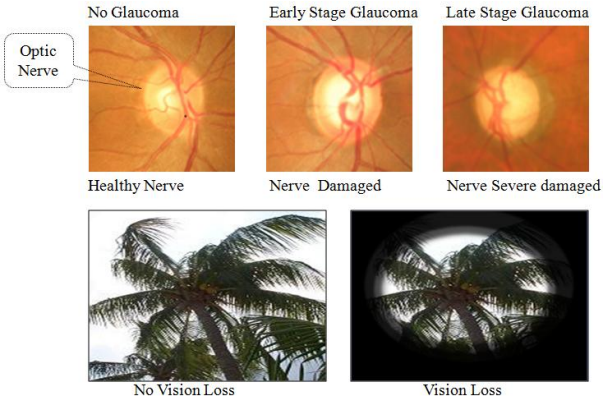

Fig. 1: The first row of the picture shows the fundus images of three patients with no glaucoma, early stage glaucoma and late stage glaucoma respectively. The second row shows what a patient can see with no vision lost and with vision lost due to glaucoma. It is clearly shown that optic nerve damage proceeds vision lost, and the method based on optic nerve damage is able to detect glaucoma earlier than functional vision test.

Corresponding author. Address: 1 Fusionopolis Way, #21-01 Connexis (South Tower), Singapore 138632
E-mail address: jliu@i2r.a-star.edu.sg (Jimmy Liu).

J. Liu, D.W.K. Wong, Z. Zhang and N.M. Tan are with the Institute for Infocomm Research, A*STAR, Singapore (email: {jliu, wkwong, zzhang, nmtan}@i2r.a-star.edu.sg)

C. Y. Cheung, M. Baskaran, T. Aung and T.Y. Wong. are with Singapore Eye Research Institute.

there remains a lack of an automatic, cost effective, sensitive and precise method to screen for glaucoma.

The 2D fundus digital image is taken by a fundus camera, which photographs the retinal surface of the eye. In comparison with OCT/HRT machines, the fundus camera is easier to operate, less costly, and is able to assess multiple eye conditions. It is widely used by optometrists, ophthalmologists, and other medical professionals for ocular disease monitoring, detection and screening.

Many researchers have utilized the fundus images to automatically analyze the optic disc structures. Some [8-13] use the single 2D fundus image (or "fundus image" in short form) or stereo images to segment the optic disc; others[14-16] use the fundus image directly to measure both the optic disc and optic cup boundaries. Among them, the ARGALI system [15] makes use of level set techniques to derive boundaries of the optic cup and disc. It calculates CDR (Cup-to-Disc Ratio) from single 2D fundus image and provides an objective and consistent measurement with potential for glaucoma screening. However, ARGALI was only tested on 104 images and the experimental result is not representative enough to analysis the glaucoma diagnosis. A-Levelset medical image segmentation algorithm further boosts level set algorithm. AGLAIA system based on A-Levelset algorithm has been tested on larger datasets with better experimental results in comparison with ARGALI. This paper analyzes the AGLAIA system using the ROC (Receiver Operating Characteristic) curve on RVGSS (Retinal Vasculature Glaucoma Subtype Study) clinical data, which consists of clinically diagnosed glaucoma and non-glaucoma cases. It is a further step toward the deployment of a fully automatic glaucoma detection system from fundus images.

II. Methods

A. CDR as an Image Cue for Glaucoma Diagnosis

The optic disc (disc) is the circular region where ganglion cell axons exit the retina to form the optic nerve. The optic cup (cup) is the depression in the center of the optic disc. The area between the optic disc and cup is called the optic neuro-retinal rim (rim), where the optical nerve resides (as shown in Fig. 2).

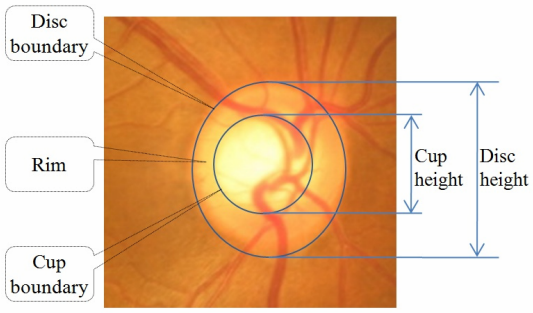

Fig. 2. Optical Disc and Optical Cup

The CDR (Cup-to-Disc Ratio) is defined as the ratio of the vertical cup height divided by the vertical disc height:

$$CDR = \frac{\text{Cup height}}{\text{Disc height}} \quad (1)$$

In order to calculate the CDR, we need to segment both the optic disc and optic cup from the fundus images. In contrast with the segmentation of the optic disc, the segmentation of the optic cup is considered [15-16] more challenging This is due to the decreased visibility of the boundary between the optic cup and the optic rim, which is often further compounded by the high density of vascular architecture near the optic cup region.

A large CDR denotes a higher risk of having glaucoma, thus automatic glaucoma diagnosis can be assisted by automatic calculating the CDR ratio, and the challenge is to segment the optic cup and disc accurately.

To formalize our discussion, we define the optic rim R(x,y) in a 2D fundus image S(X,Y) as the area where the optic nerve resides:

$$R(x, y) = \{(x, y) \mid x \in X; y \in Y; (x, y) \text{ optic nerve exisits at } (x, y)\}. \quad (2)$$

The optic disc *D(x,y)* contour can thus be understood as the outer boundary of the optic rim:

$$D(x, y) = \{ k(x, y) \mid (x, y) \in R; \; k \text{ resides on the outer boundary of the optic rim R} \} \quad (3)$$

In RGB space, a point k in D can be denoted by their red/green/blue triplet color codes at the point as (k_r, k_g, k_b). Our previous works [15.16] show that the red channel is better in distinguishing the disc boundary.

The optic cup *C (x,y)* contour is defined as:

$$C(x, y) = \{ j(x, y) \mid (x, y) \in R; \; \text{j resides on the inner boundary of the optic rim R} \}. \quad (4)$$

The disc area *Da* and cup area *Ca* are defined as the areas enclosed by the disc contour *D (x,y)* and cup contour *C (x,y)*.

In RGB space, a point j in C(x,y) can be denoted by their red/green/blue triplet color codes at the point as (j_r,j_g,j_b). Our previous works [15.16] also show that the blue or green channels are better in distinguishing the cup boundary.

Finding the optic disc contour *D(x,y)* can be understood as a fundus image segmentation issue, in which the optic disc segmentation is to find the closed contour (boundary) between the optic rim and retina (inside is the rim and outside is the retina). If the signed distance function $f_d(x,y)$ is used to determine the closeness of a given point *(x,y)* in the fundus image is to *D(x,y)*, a positive value indicates that the point *(x,y)* is inside *Da*, value zero indicates the point *(x,y)* is part of *D(x,y)*, a negative value indicates the point *(x,y)* locates

outside of Da

$$f_d(x,y)=\begin{cases} dist((x,y),Da) & if\ (x,y)\in Da \\ 0 & if\ (x,y)\in D \\ -dist((x,y),Da) & \text{if } (x,y)\notin Da \end{cases}. \quad (5)$$

where $dist((x,y),Da)=\inf(dist((x,y),z);z\in \mathrm{Da}$, and inf the infimum function.

Similarly, identifying the optic cup contour *C(x,y)* can be understood as a segmentation issue as well, the cup segmentation is to find the closed contour between the optic rim and the central depression cupping area. The signed distance function for cup segmentation f_c *(x,y)* can be described as:

$$f_c(x,y)=\begin{cases} dist((x,y),Ca) & if\ (x,y)\in Ca \\ 0 & if\ (x,y)\in C \\ -dist((x,y),Ca) & \text{if } (x,y)\notin Ca \end{cases}. \quad (6)$$

Where $dist((x,y),Ca)=\inf(dist((x,y),z);z\in \mathrm{Ca}$,

The disc and cup segmentation can be described as finding the solutions for the function f_d and f_c while satisfying the constraint $C \subseteq D$.

In the following sections, we discuss our algorithm on optic cup segmentation and the same approach can be applied to the optic disc segmentation.

B. Deformable Models for Fundus Image Segmentation

Deformable model, as the name implies, involves deformation of an initial estimate and a deformable template, to finally reach the boundary (contour) of the target object. Applying it in fundus medical image segmentation, we need to do an initial estimate of the desired target contour, which is subsequently moved by image driven forces to the boundaries of the tissue. Two types of forces jointly decide the final boundary. The internal force, defined within the curve, keep the model smooth during deformation; whereas the other external forces, computed from the underlying medical image data, move the model toward the object boundary within the fundus medical image.

There are parametric and none-parametric deformable models. In the parametric form like ASM (Active Shape Model) [17] or SNAKE [18], an explicit parametric representation of the curve is constructed and deformed to fit the target object. ASM can achieve good results in disc segmentation. However, this form severely restricts the degree of topological adaptability of the model, especially if the deformation involves splitting or merging (which happens often in the optic disc/cup regions in fundus images, where blood vessel and pathologies are often interweaved with the surrounding tissue).

Parametric implicit deformable models such as level-set [19], optimize the shape globally to handle topological changes. The level-set based ARGALI system [15] has been developed to segment optic disc and optic cup from fundus images. However, level set algorithm often relies on a priori knowledge about the respective anatomy [7]. They are not robust to boundary gaps and handling local deformation. These can lead to leaking in the optic cup segmentation, especially in the temporal side, where the cup boundary is not clearly defined. To overcome the limitation of the level set-based algorithm in optic disc and optic cup segmentation, A-Levelset cascades Level set and ASM algorithm by using ASM to fine-tune the outcome of the level set algorithm. A-Levelset is applied in optic disc and cup segmentation to detect glaucoma in AGLAIA and it achieves promising experimental results.

III. Results and Discussions

We run both ARGALI and AGLAIA on a Dell Precision T3500V Workstation and tested the systems on the RVGSS dataset, which consists of 66 glaucoma confirmed cases and 225 non-glaucoma cases collected from the Singapore National Eye Center. The average running time for segmenting the cup/disc boundary and calculating the CDR is 5 seconds for ARGALI and 7.4 seconds for AGLAIA.

Using the clinical ground truth marked by the glaucoma specialists, Table 1 compares CDR measurement error rates and shows that AGLAIA outperforms ARGALI. AGLAIA reduces ARGALI's CDR measurement mean absolute error from 0.36 to 0.21 and the mean square error from 0.17 to 0.07 on RVGSS dataset. Furthermore, AGLAIA's mean absolute error rate is comparable with the inter- and intra-observer variability rates, which stands at 0.2 and 0.15 respectively [6].

TABLE I
CDR Measurement Error Rates of ARGALI and AGLAIA on RVGSS

Method	Error Assessment	Measurement Error Rates
ARGALI	Mean Square Error	0.17
	Mean Absolute Error	0.36
AGLAIA	Mean Square Error	0.07
	Mean Absolute Error	0.21

To evaluate the capability of AGLAIA and ARGALI in diagnosing glaucoma using CDR, we need to look at the ROC curves of both systems. Fig. 3 shows the ROC curves of the two approaches, and it can be observed that AGLAIA (green curve) is able to boost the Area Under the Curve from ARGALI's (blue curve) 0.42 to 0.73. The ROC curves also show that AGLAIA is able to achieve better sensitivity and specificity distribution than ARGALI in CDR based glaucoma diagnosis. However, it is also shown that there is still a big gap between the automatic system's performance and the human experts' performance (the clinical Area Under the Curve for human expert on RVGSS is 1.0).

Using CDR as the only risk factor, AGLAIA is able to

achieve 0.73 Area Under the Curve and the CDR accuracy

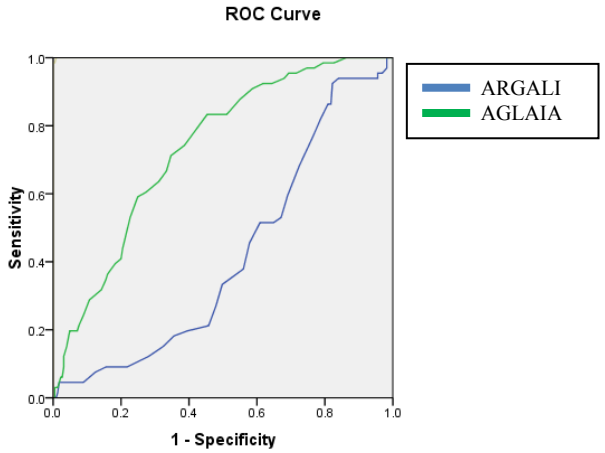

Fig. 3. ROC curves of ARGALI and AGLAIA for glaucoma diagnosis.

rate comparable with the inter-observer error range. Even though the performance is still far from perfect, the result is subjective, consistent and fast. It does not rely on trained glaucoma specialists or specialized and costly OCT/HRT machines. This shows potential to use automatic assessment based on fundus image as a means to screen for glaucoma. Research is currently underway to use other image cues like vessel kinking, disc hemorrhage, PPA and cup notching to further boost the system performance. It is expected that fusing those image cues with the CDR can further boost the ROC curves in glaucoma diagnosis.

In the future, we intend to further improve the accuracy and conduct test on larger clinical databases. The objective of the work is to use advances in medical image processing and utilize 2D fundus images to screen for glaucoma at the primary healthcare clinics

IV. Conclusions

AGLAIA is able to boost the performance of level set based ARGALI system in automatic CDR measurement. The experimental results conducted on a clinical dataset demonstrate the potential to screen or diagnose glaucoma objectively using widely available fundus images automatically. It is a further step toward deployment of fully automatic glaucoma diagnosis system from fundus images.

References

[1] B. E. Klein, *et al.*, "Prevalence of glaucoma. The Beaver Dam Eye Study," *Ophthalmology,* vol. 99, pp. 1499-504, Oct 1992

[2] H. A. Quigley and A. T. Broman, "The number of people with glaucoma worldwide in 2010 and 2020," *Br J Ophthalmol,* vol. 90, pp. 262-7, Mar 2006.

[3] T. Damms and F. Dannheim, "Sensitivity and specificity of optic disc parameters in chronic glaucoma," *Invest Ophthalmol Vis Sci,* vol. 34, pp. 2246-50, Jun 1993.

[4] N. R. Rylander and S. D. Vold, "Cost analysis of glaucoma medications," *Am J Ophthalmol,* vol. 145, pp. 106-13, Jan 2008.

[5] S. Y. Shen, *et al.*, "The prevalence and types of glaucoma in malay people: the Singapore Malay eye study," *Invest Ophthalmol Vis Sci,* vol. 49, pp. 3846-51, Sep 2008.

[6] R. Varma, *et al.*, "Agreement between Clinicians and an Image Analyzer in Estimating Cup-to-Disc Ratios," *Archives of Ophthalmology,* vol. 107, pp. 526-529, Apr 1989.

[7] I. Dielemans, *et al.*, "The prevalence of primary open-angle glaucoma in a population-based study in The Netherlands. The Rotterdam Study," *Ophthalmology,* vol. 101, pp. 1851-5, Nov 1994.

[8] A. Hoover and M. Goldbaum, "Locating the optic nerve in a retinal image using the fuzzy convergence of the blood vessels," *Ieee Transactions on Medical Imaging,* vol. 22, pp. 951-958, Aug 2003.

[9] M. Niemeijer, *et al.*, "Segmentation of the optic disc, macula and vascular arch in fundus photographs," *Ieee Transactions on Medical Imaging,* vol. 26, pp. 116-127, Jan 2007.

[10] X. Zhu and R. M. Rangayyan, "Detection of the optic disc in images of the retina using the Hough transform," *Conf Proc IEEE Eng Med Biol Soc,* vol. 2008, pp. 3546-9, 2008.

[11] H. Li and O. Chutatape, "Boundary detection of optic disk by a modified ASM method " *Pattern Recognition,* vol. 36, pp. 2093-2104, 2003.

[12] J. Xu, *et al.*, "Optic disk feature extraction via modified deformable model technique for glaucoma analysis," *Pattern Recognition,* vol. 40, pp. 2063-2076, Jul 2007.

[13] M. D. Abramoff, *et al.*, "Automated segmentation of the optic disc from stereo color photographs using physiologically plausible features," *Investigative Ophthalmology & Visual Science,* vol. 48, pp. 1665-1673, Apr 2007

[14] G. D. Joshi, *et al.*, "Vessel Bend-Based Cup Segmentation in Retinal Images," in *Pattern Recognition (ICPR)*, Hyderabad, India, 2010.

[15] J. Liu, *et al.*, "ARGALI : An Automatic Cup-to-Disc Ratio Measurement System for Glaucoma Analysis Using Level-set Image Processing," *13th International Conference on Biomedical Engineering, Vols 1-3,* vol. 23, pp. 559-562 2303, 2009

[16] D. K. Wong, *et al.*, "Automated detection of kinks from blood vessels for optic cup segmentation in retinal images," in *SPIE* FL, USA 2009.

[17] T. F. Cootes, *et al.*, "Active Shape Models - Their Training and Application," *Computer Vision and Image Understanding,* vol. 61, pp. 38-59, Jan 1995.

[18] M. Kass, *et al.*, "Snakes - Active Contour Models," *International Journal of Computer Vision,* vol. 1, pp. 321-331, 1987.

[19] S. Osher and J. A. Sethian, "Fronts Propagating with Curvature Dependent Speed: Algorithms Based on Hamilton-Jacobi Formulations," *JOURNAL OF COMPUTATIONAL PHYSICS,* vol. 79, pp. 12--49, 1988.